A Unique Petrified Tree Fern from Northeast China

Ying Yan, Xiao-Yan Yu, Han-Yue Xu, and Zhi-Rong Xie

A unique petrified tree fern displaying distinct patterns was recently discovered in northeast China, attracting considerable interest. This study provides a comprehensive set of data for this material obtained through standard gemological testing, petrographic observation, scanning electron microscopy, energy-dispersive spectroscopy, electron probe microanalysis, and Raman spectroscopy. The petrified tree fern exhibits colors ranging from golden yellow to brown, with additional variations caused by iron oxides. Chalcedony is the primary mineral component, while the presence of metastable moganite gives chalcedony its fibrous nature, contributing to the delicate structure of the samples. The surface pattern originates from plant structures preserved during silicification, further confirming the samples belong to the extinct Cretaceous period tree fern *Tempskya* sp.

Petrified wood is the fossilized remains of ancient trees that have undergone a process occurring over millions of years (Nowak et al., 2005; Yoon and Kim, 2008; Kim et al., 2010). During this process, dissolved SiO_2 infiltrates the organic matter of buried trees, causing the precipitation of various crystalline siliceous minerals along the wood fiber cells. As a consequence, silicified fossils with preserved woody structures are formed (Murata, 1940; Rößler, 2000; Mustoe, 2008; Yu, 2016). However, most petrified wood is not of gem quality, lacking the necessary beauty and luster (Saminpanya, 2015).

Since 2010, a unique tree fern fossil recovered from riverbeds and secondary placers in northeast China has captured the attention of botanists (Cheng and Liu, 2017; Yang et al., 2018). This unusual tree fern, *Tempskya*, is the only genus in the family Tempskyaceae and occurred only in the Cretaceous (box A). These petrified tree fern fossils are composed of polycrystalline quartz. With its distinct patterns, this material has drawn the interest of gem collectors in the area (Xu, 2021). Lapidary artists value specimens for their use in cabochons, beads, and carvings (figure 1). As local jewelers recognized the worth of this material, they began to incorporate it into souvenirs and polished collectible items, adding to the appreciation of petrified tree fern (Pakhomova et al., 2020).

Figure 1. Chalcedony petrified tree fern is carved as an ornamental gem material. This 60 × 40 mm dragon carving has a uniform texture and bright color. Photo by Hai-Long Wang.

See end of article for About the Authors and Acknowledgments.
Gems & Gemology, Vol. 59, No. 4, pp. 450–465,
http://dx.doi.org/10.5741/GEMS.59.4.450

Box A: Botany of Petrified Tree Fern

Tree ferns, members of the Cyatheales order, constitute a captivating and ancient group of ferns distinguished by their unique and primitive traits. These remarkable ferns stand apart from their botanical counterparts in several ways (Large and Braggins, 2004):

1. *Trunk-like stems:* Living tree ferns are primarily recognized for their upright, trunk-like stems, which resemble the trunks of trees. These stems can grow to considerable heights, and they are a defining feature of these ferns.
2. *Large compound leaves:* At the top of their tall stems, tree ferns display large and elaborate compound leaves. These leaves consist of numerous leaflets arranged in a feather-like or palmate fashion, giving them a distinctive and attractive appearance.
3. *Primitive nature:* Tree ferns are considered relatively primitive in the plant kingdom. Their status as "living fossils" and the distinctive features of their stems and growth habits make tree ferns a captivating subject of study in the field of botany.

Tempskya, an extinct genus of tree ferns, thrived during the Cretaceous period and has left fossils in both the Northern and Southern hemispheres (Tidwell et al., 2010). Unlike living tree ferns, *Tempskya* was characterized by short, slender underground stems or rhizomes with diminutive leaves (figure A-1). Its growth habit, distinct from any contemporary fern or living plant, consisted of multiple conjoined dichotomous branching stems enmeshed within roots to form a "false trunk" (Martínez and Olivo, 2015). The "false trunk" was composed of rhizomes modified to grow vertically and embedded in a dense mantle of adventitious roots. The trunk cross sections produced an attractive pattern of light and dark tissues originating from the vascular system of stem and leaf traces (figure A-2). During the process of silicification, the tree fern underwent a transformation that left the stone with a beautiful pattern of color and texture.

Figure A-1. Tempskya *sp. reconstruction. Illustration by Matteo De Stefano/MUSE; courtesy of MUSE - Science Museum of Trent in cooperation with Wikimedia Italia.*

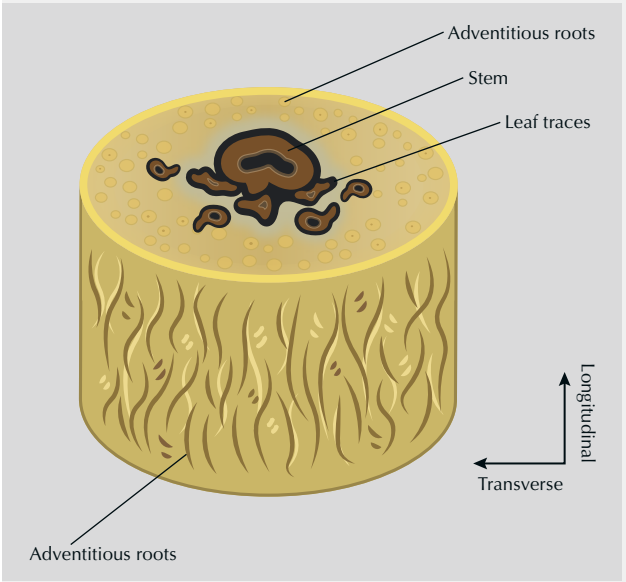

Figure A-2. Anatomy of petrified tree fern Tempskya *sp. The longitudinal and transverse sections of the trunk produce unique patterns of light and dark tissues originating from the vascular system of the stem, adventitious roots, and leaf traces. Within the realm of botany, a plant's vascular system is the assemblage of conducting tissues and associated supportive fibers that transport nutrients and fluids throughout the plant body. Illustration by Ying Yan.*

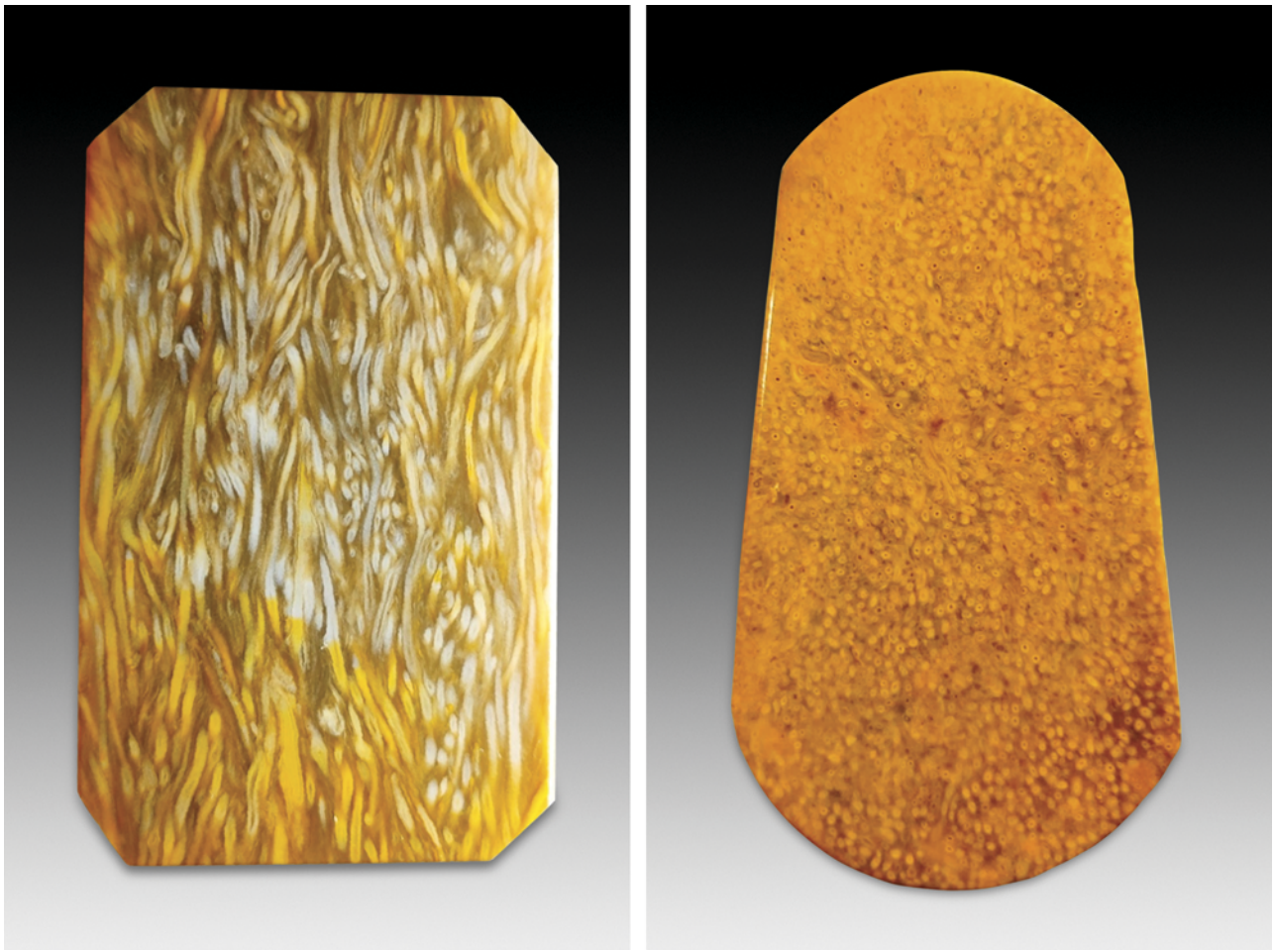

Figure 2. These polished slabs of petrified tree fern with an attractive golden yellow color show two different unusual plant textures that are typical of fine Chinese material. The entangled adventitious roots form a vivid pattern in a longitudinal section (left, 55 × 35 mm). Many adventitious roots have a circular shape in cross section (right, 40 × 25 mm). Photos by Hai-Long Wang.

Petrified tree fern possesses desirable qualities as a gem material, characterized by its refined texture and preserved plant patterns (figure 2). Previous studies have focused primarily on paleogeography, paleoclimatology, and mineralogical aspects of petrified tree fern (Rößler, 2000; Witke et al., 2004), leaving its gemological significance largely unexplored, particularly with regard to microstructural analysis. The resemblance between petrified tree fern and tiger's-eye (Holden, 2003) raises the need for accurate separation (figure 3). In view of these considerations, this study provides a comprehensive analysis of the microstructure and mineral composition of petrified tree fern.

MATERIALS AND METHODS

Six studied petrified tree fern samples (S1–S6) were procured from the gem market in Qiqihar, Heilongjiang Province, China. These specimens were originally collected by local villagers from fluvial deposits near the village of Henan, Keshan County, in Heilongjiang Province in the northern Songliao Basin (figure 4). The Songliao Basin is a Mesozoic-Cenozoic

In Brief

- Petrified tree fern displays a typical golden yellow to brown color and distinct plant structures such as stems, adventitious roots, and leaf traces.
- The plant patterns preserved during silicification indicate the specimens in this study belonged to the extinct Cretaceous tree fern *Tempskya* sp.
- Fibrous chalcedony is the primary mineral contributing to the delicate structure of petrified tree fern.

Figure 3. Brownish yellow tiger's-eye sold in the jewelry market in Wuhan, China, is identified incorrectly as petrified tree fern. The tiger's-eye is in the cross pattern and in the upper right, alongside various other products sold at the market. Photo by Ying Yan.

intracratonic basin across the Heilongjiang, Jilin, and Liaoning provinces of northeast China. One of the most prolific oil sedimentary basins in China, it is considered a long-lived terrestrial basin preserving a nearly complete Cretaceous sedimentary record (Yang et al., 2018). The Cretaceous strata in the basin are rich in biological fossils (Gao and Song, 1994; Kong et al., 2006). A discovery there in 2017 of a new species of tree fern fossil, *Tempskya zhangii*, has shed light on the paleogeographic environment of the Songliao Basin during the Cretaceous period (Yang et al., 2018).

The rough samples were rounded chunks covered with gray-white and brownish yellow weathering crust, indicating that the fossils had been transported by water over a long distance to their current sites (figure 5). The six samples were ground into polished slabs in the transverse direction (figure 6). Additionally, a sample of tiger's-eye with an appearance similar to that of petrified tree fern was procured from

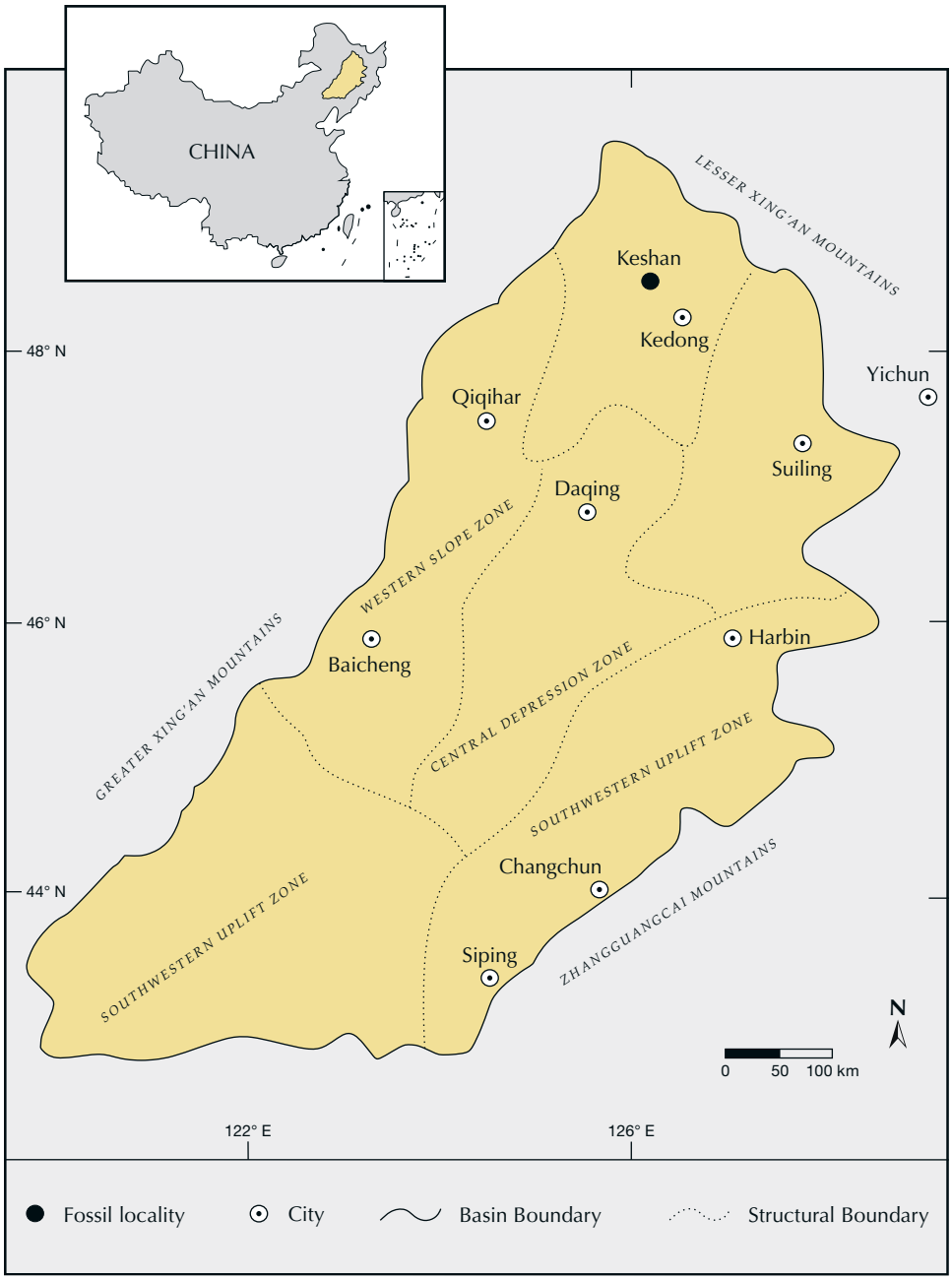

Figure 4. This map of Songliao Basin of northeast China shows fossil localities and major structure zones. Modified from Cheng and Liu (2017).

the jewelry market in Wuhan for gemological and visual comparisons (figure 7).

The six petrified tree fern samples and the one tiger's-eye sample were examined using standard gemological methods including visual observation, refractive index measurement, fluorescence reaction observation under long-wave (365 nm) and short-wave (254 nm) UV, and hydrostatic specific gravity testing.

The samples were prepared as thin sections both perpendicular and parallel to the plant texture direction, labeled as transverse and longitudinal, respectively. These sections were examined using an Olympus BX51 petrographic microscope. Scanning electron microscopy (SEM) was used to observe fractures in randomized directions of the petrified tree fern samples, performed by JEOL JSM-7800F. Working voltage and working distance were 15 kV and 10 mm, respectively. Energy-dispersive spectrometry (EDS) (Oxford X-Max 50) element mapping allowed the observation of chemical variation within the same regions.

Figure 5. The six rough samples of petrified tree fern from northeast China investigated in this work, ranging from 135.50 to 332.13 g. Photos by Han-Yue Xu.

Chemical composition was determined at the MNR Key Laboratory of Metallogeny and Mineral Assessment, Institute of Mineral Resources, Chinese Academy of Geological Science in Beijing. The analy-

Figure 6. The six petrified tree fern samples cut in the transverse direction and analyzed for this study (3.2–4.1 cm in length and 1.6–2.5 cm in width). Photos by Han-Yue Xu.

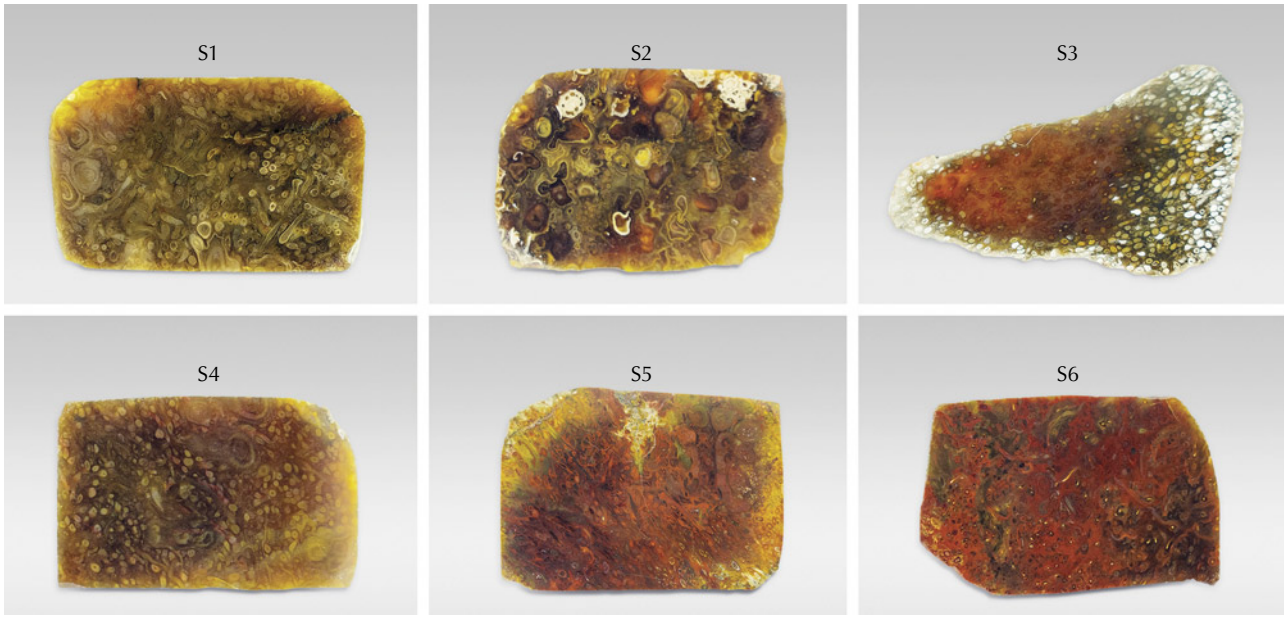

Figure 7. This polished specimen of tiger's-eye (3.5 × 1.6 mm, 14.57 g) exhibits a golden yellow coloration similar to that of petrified tree fern. Photo by Ying Yan.

sis was performed with a JEOL JXA-8230 electron probe microanalyzer (EPMA) equipped with four wavelength-dispersive spectrometers. The sections were coated with an approximately 20 nm thin conductive carbon film prior to analysis. Accelerating voltage, beam current, and spot size were 15 kV, 20 nA, and 5 µm, respectively. Jadeite (silicon, aluminum), hematite (iron), rutile (titanium), potassium feldspar (potassium), and wollastonite (calcium) were used as standards. Data were corrected online using a modified ZAF correction procedure.

Raman spectra were recorded using a Horiba HR-Evolution Raman micro spectrometer with an argon-ion laser operating at 532 nm excitation between 1800 and 100 cm^{-1} and accumulating up to three scans.

RESULTS

Gemological Properties and Visual Appearance. The gemological properties of the six petrified tree fern samples are compared to the single tiger's-eye sample in table 1. All of the samples displayed golden yellow to brown colors, but red impurities were observed in regions of samples S5 and S6. All petrified tree fern samples had a refractive index of 1.53–1.54 with specific gravity varying from 2.60 to 2.63. Their luminescence was inert under long-wave and short-wave UV radiation.

The polished surface of the petrified tree fern highlighted the internal structure of the plant, which differed from the parallel fiber structure found in tiger's-eye. Three representative samples with distinctive internal textures of tree fern were selected for visual examination (figure 8). The unique surface patterns consisted of plant stems, adventitious roots, and leaf traces, appearing striped in a longitudinal section or irregularly rounded in a transverse section. The plant texture of sample S5 was entirely red, with tubular stems, dense adventitious roots, leaf bases,

Figure 8. The structures of samples S1 (A), S2 (B), and S5 (C) observed under visible light. A is a longitudinal cross section view; B and C are transverse cross section views. Photomicrographs by Han-Yue Xu; field of view 2.0 mm.

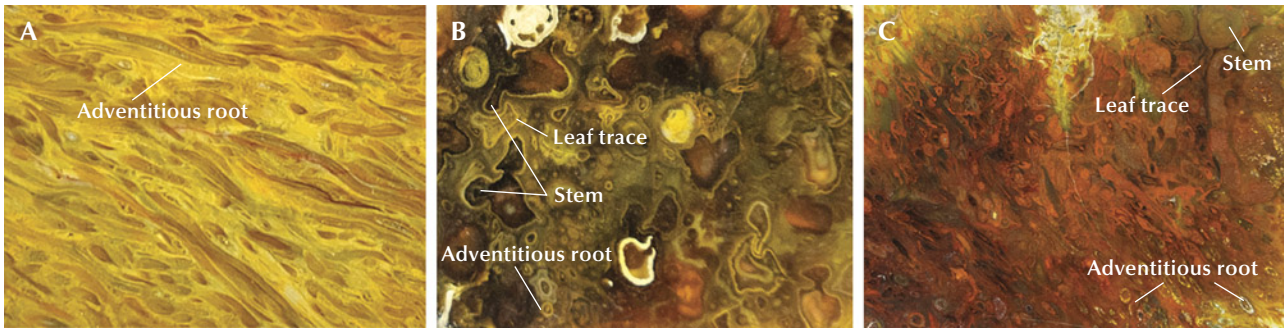

TABLE 1. Gemological properties of petrified tree fern and tiger's-eye from China.

Property	Petrified tree fern	Tiger's-eye
Color	Golden yellow, brown, and red band; gray-white regolith on the surface	Golden yellow to brown
Diaphaneity	Translucent to opaque	Opaque
Refractive index[a]	1.53–1.54	1.54
Specific gravity	2.60–2.63	2.60
Long-wave UV	Inert	Inert
Short-wave UV	Inert	Inert
Textural features observed in visible light	Individual stems, adventitious roots, and leaf traces give the petrified specimens a unique appearance	The lustrous golden brown band exhibits radiant chatoyancy in polished sections

[a]*Determined using the spot method.*

and a clear entanglement. Conversely, tiger's-eye is characterized by lustrous golden brown bands that display banded chatoyancy (figure 9).

Figure 9. Chatoyancy in a polished section of tiger's-eye. A characteristic of this gem is the local variability in the orientation of the cat's-eye, causing different bands of reflected light when rotated relative to a point light source. Photomicrograph by Ying Yan; field of view 1.3 mm.

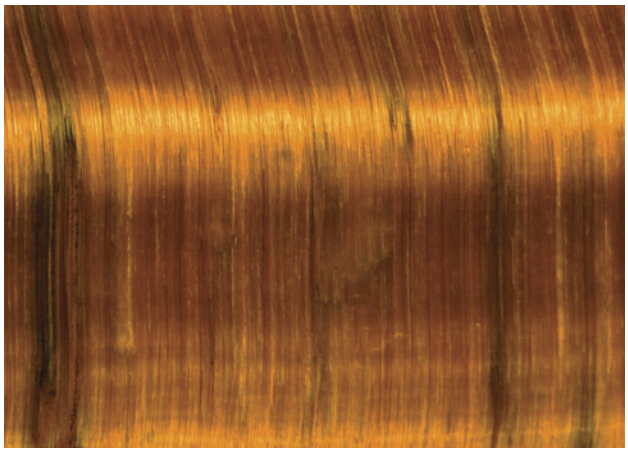

Microstructure. A polarizing microscope further revealed a well-preserved wood grain structure in the petrified tree fern samples. Individual stems were tubular and contained pith, vascular strands, xylem (the primary vascular tissue, which transports water and dissolved minerals from the roots to the leaves), and a cortex (figure 10A). The cortex was three-layered (figure 10B); the middle cortex had thick wall cells, while the outer and inner cortex were relatively thin. The pith was composed of thin wall cells that were elliptical in cross section. Each leaf trace had a single spindle-shaped vascular bundle (specialized tissues that run through and carry water and nutrition to different parts of the plant). The adventitious root was small in diameter, and the xylem was differentiated into two zones. The outer cortex consisted of large parenchyma cells. In contrast, the inner cortex was composed of thin wall cells (figure 10C). The solid, compact trunk was composed of stems embedded in a matrix of adventitious roots that were independent and intertwined with other roots (figure 10D).

Mineralogically, the microcrystalline structure of petrified tree fern is diverse. Thin sections showed that samples were silicified by replacement, and

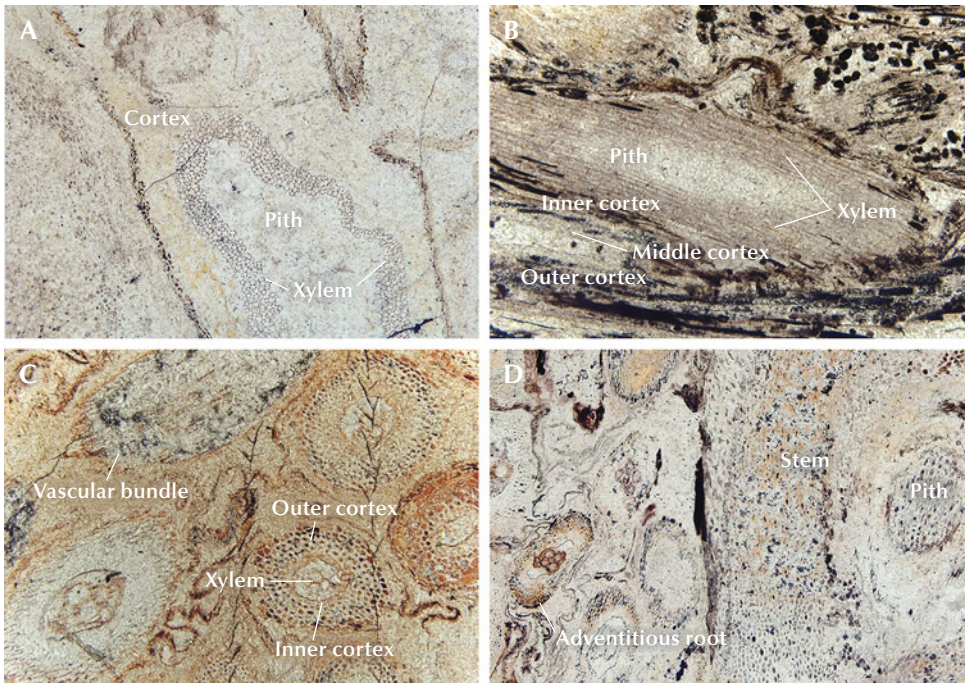

Figure 10. Typical plant structure characteristics of petrified tree fern under plane-polarized light. A: In a cross section of S2, a stem segment shows cortex, xylem, and pitch. B: In a longitudinal section of S3, the stem, a visible three-layered cortex, and pith are surrounded by xylem. C: Details of the diarchal xylem and the outer and inner cortex of an adventitious root in S4. D: A cross section of S5 shows a comparison of stem and adventitious root structure. Adventitious roots are small in diameter and appear curved, round, or oval. Photomicrographs by Han-Yue Xu; fields of view 0.48 mm (A, B, and D) and 0.36 mm (C).

chalcedony ± microcrystalline quartz made up more than 95% of their content. The quartz particles were rarely euhedral, mainly presenting as irregular microcrystals (less than 10 μm in diameter) and fibrous chalcedony spherulites (100–200 μm in diameter). The quartz particles were grayish white under plane-polarized light. According to Li (2016), wood fiber is the plant tissue component that is most resistant to decomposition and recrystallization, making it hard to mineralize. We therefore conclude that brownish yellow wood fiber structures are partly preserved in the petrified tree fern (figure 11A), but the decom-

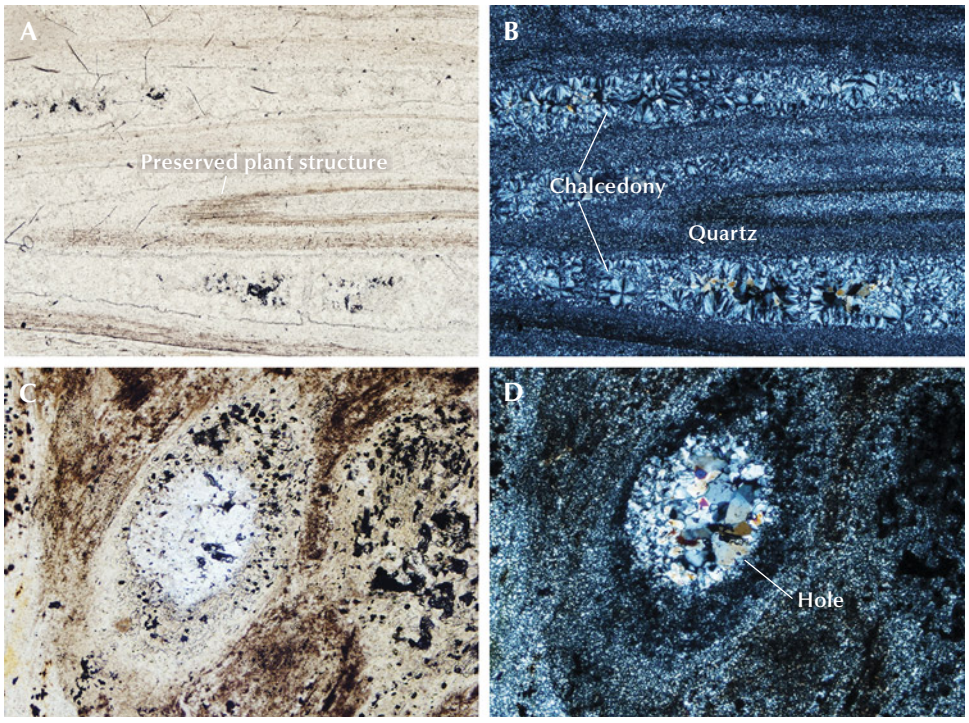

Figure 11. Photomicrographs of petrified tree fern taken with a polarizing microscope. A: Plane-polarized light reveals the preserved yellow-brown plant structure in S2. B: Cross-polarized light shows that the vein is filled with a mixture of chalcedony and microcrystalline quartz. C: A hollow structure image of sample S4 under plane-polarized light. D: Cross-polarized light reveals that subhedral quartz crystals precipitated in the hole, while fine-grained quartz surrounded the hole. Photomicrographs by Han-Yue Xu; fields of view 0.55 mm (A and B) and 0.43 mm (C and D).

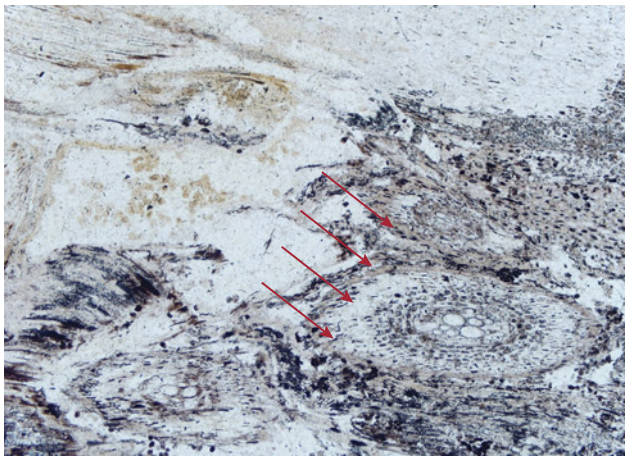

Figure 12. In sample S5, the plant structure features become more evident closer to the regolith, following the direction of the arrows. Photomicrograph by Han-Yue Xu; field of view 0.8 mm.

posed part of the plant structure filled with chalcedony (figure 11B). In general, fossilization occurs when quartz has precipitated on the wall cells of samples, while chalcedony forms in open spaces such as vessels and veins (Hassan, 2017). As shown in figure 10B, fine-grained quartz filled in areas where woody structures were retained in the plant stems and roots. Conversely, radiating fibrous chalcedony crystallized in veins. Moreover, the subhedral quartz crystals were present in hollow structures such as vessels, veins, and holes (figure 11, C and D), while fine-grained quartz surrounded the hole.

In addition, the plant structure was more evident near the shell of the petrified tree fern (figure 12) due to surface weathering. This weathering leads to fine crystalline decomposition and recrystallization of silica along the woody texture, reducing transparency and enhancing the distinct wood structure. The secondary regolith of the samples exhibited a wide distribution of yellow and red minerals that are associated with the woody structure (figure 13). However, the coloration is mainly affected by various minerals present during the weathering process.

SEM imaging revealed three distinct quartz textures in sample S4. The first texture consisted of cryptocrystalline quartz particles of 1 μm in diameter, grown in layers. The second was characterized by euhedral equant quartz crystals with particle diameters ranging from 1 to 5 μm (figure 14A), filling voids and partially visible due to a rhombohedral fracture surface. The first and second textures were both granular structures with low transparency. Conversely, the third texture contained semitranslucent regions composed of chalcedony fibers measuring approximately 5–10 μm in length. Figure 14B illustrates the structural characteristics of fibrous chalcedony. Most of the silica particles in the samples consisted of fine-grained quartz and chalcedony, with euhedral particles being less common.

The occurrence of vascular bundle structures on certain fracture surfaces mainly indicated atypical growth textures. Dense, oriented fibrous chalcedony formed around the pore wall. In the cross section of

Figure 13. Impurity minerals surrounded by the weathered shell of S5 and S6, respectively. Left: These yellow color iron compounds were not positively identified by Raman spectroscopy. Right: Hematite was identified using Raman analysis. Photomicrographs by Han-Yue Xu; fields of view 0.10 mm (left) and 0.48 mm (right).

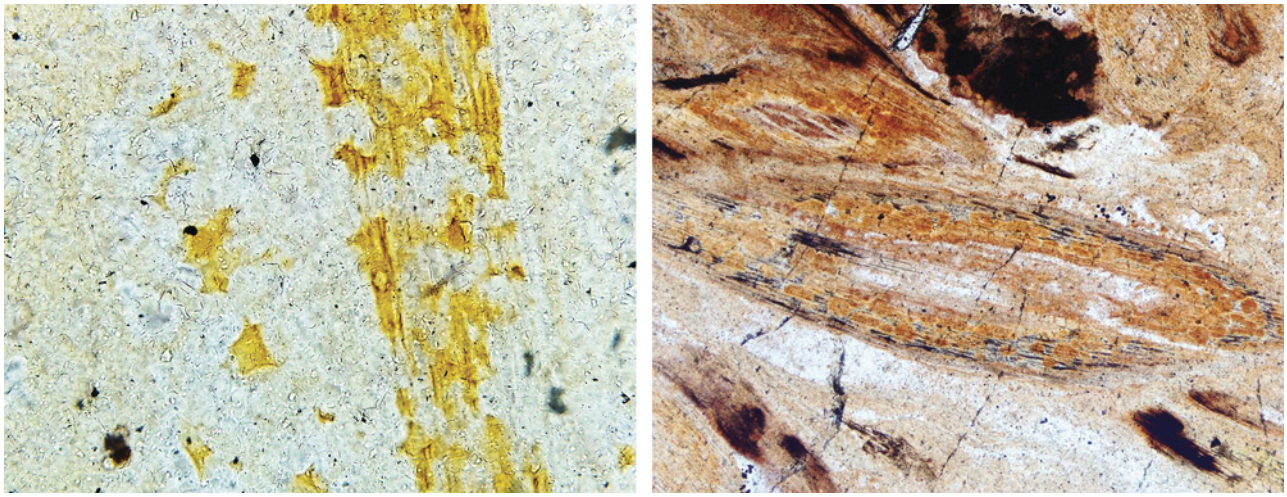

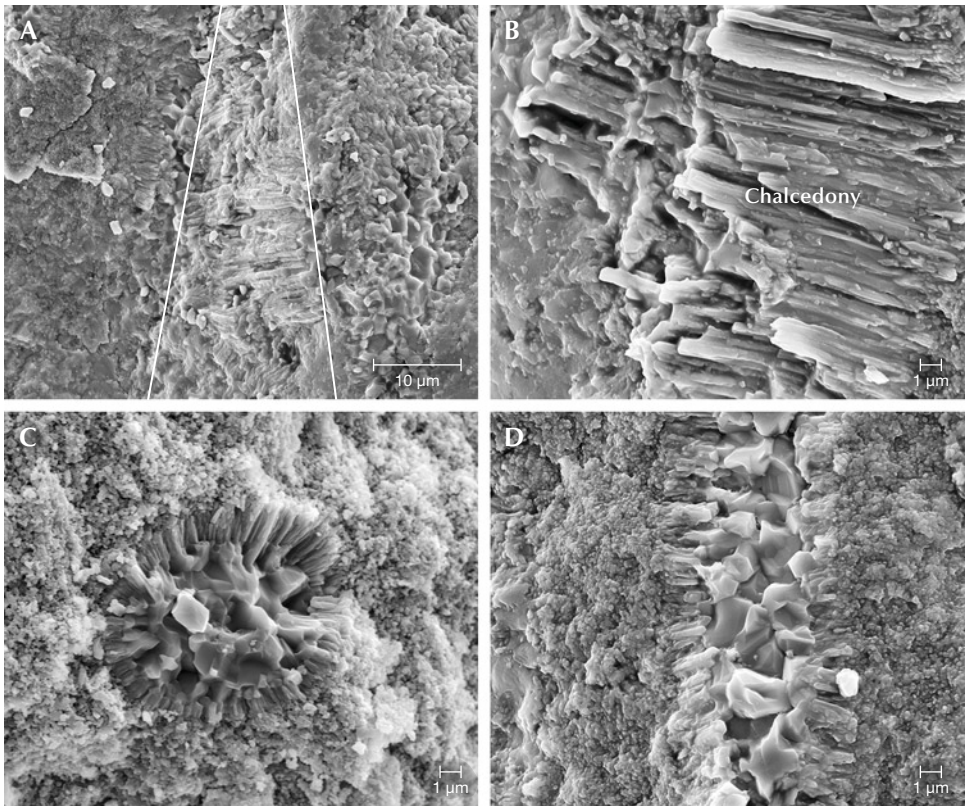

Figure 14. SEM images of petrified tree fern sample S4. A: From left to right, the contrast of mineral particle morphology between fine-grained quartz and fibrous quartz is indicated by the white lines. B: Details of the fibrous chalcedony in image A. C: The silica occurs as radial arms, as shown in cross section. D: In a longitudinal section, the minerals show a parallel arrangement, with the crystals appearing to develop from the outside to the inside.

sample S4, a radial arrangement of fibers was evident (figure 14C). The vascular bundle structure showed a parallel arrangement in a longitudinal section (figure 14D). The agate-like geode growth structure suggests a silicification sequence from the outside (Scurfield and Segnit, 1984). After the SiO_2 solution or colloid enters the vascular bundle cell or duct, quartz crystals grow in an oriented pattern around the cell wall. Crystal particles become progressively larger toward the center, displaying well-defined faces, which suggests that quartz had space for growth during formation, and crystals appeared to develop inward from the exterior.

Element Mapping and Chemical Composition. In a backscattered electron image, a long columnar-shaped impurity in sample S6 can be seen in stark contrast to the host material (figure 15A). Element

Figure 15. Element mapping of sample S6 using SEM-EDS. A: A long square columnar disseminated mineral showing high contrast. B: Element mapping of the sample for silicon, iron, oxygen, calcium, and carbon.

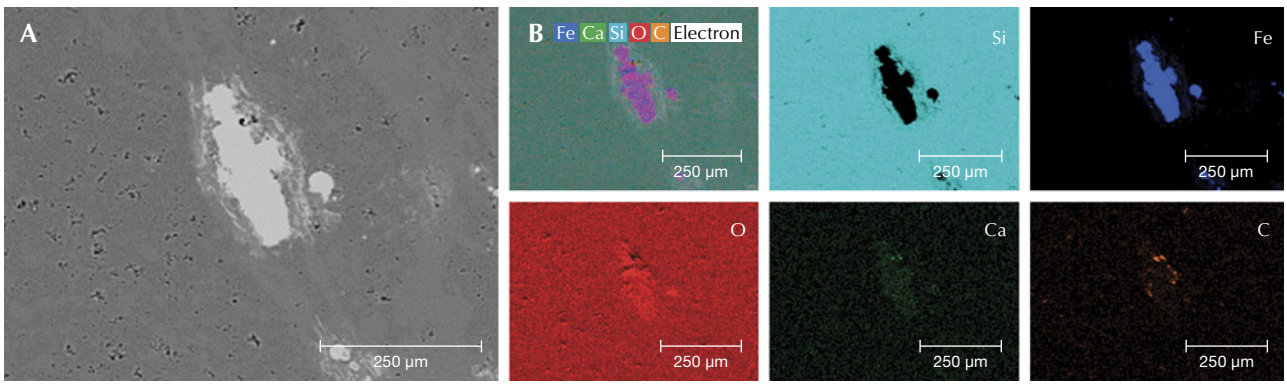

TABLE 2. Chemical composition (in wt.%) of petrified tree fern, obtained by EPMA.

Spot no.	SiO_2	Al_2O_3	FeO	TiO_2	K_2O	CaO	Total
1	99.43	0.16	0.30	0.05	0.02	0.02	99.98
2	97.94	0.10	0.01	0.02	0.02	0.01	98.10
3	98.82	0.02	0.05	0.02	0.02	0.03	98.96
4	98.68	0.16	0.14	0.13	0.01	0.02	99.14
5	99.31	0.18	0.05	0.05	0.03	0.03	99.65
Detection limit (wt.%)	0.008	0.008	0.009	0.024	0.005	0.006	

mapping revealed that the petrified tree fern matrix mainly contained silicon and oxygen, while the impurity minerals primarily consisted of iron and oxygen (figure 15B). Iron in the form of hematite is most likely the cause of color. At the same time, the boundary between the impurity minerals and the matrix contained a small amount of carbon corresponding to the residual carbonaceous matter in petrified wood (Li, 2016).

The backscattered electron image of the petrified tree fern shows a smooth surface. Five random spots on representative sample S1 were analyzed by EPMA. The results in table 2 agree well with the element mapping data, mainly containing SiO_2 (97.94–99.43 wt.%) and a few impurity elements. This confirms that there is no clear difference in the position and composition of distinct plant textures in petrified tree fern.

Raman Spectroscopy. Raman spectroscopy was used to detect other phases that might be present in the samples (Kingma and Hemley, 1994). Figure 16 reveals that the Raman spectrum of petrified tree fern sample S2 is characterized by quartz mixed with moganite, indicated by the peak at 503 cm^{-1} (Heaney and Post, 1992; Hardgrove and Rogers, 2013). The Raman shifts present in petrified tree fern and tiger's-eye occur predominantly at 127, 209, 262, 357, 402, and 465 cm^{-1}, corresponding to quartz. Specifically, the scattering peak at 465 cm^{-1} is sharp and strong, related to the typical Si–O bending vibration of quartzite. Two peaks near 127 and 209 cm^{-1} correspond to the rotational or translational vibration of SiO_4. Absorptions with very weak intensity at 262, 357, and 402 cm^{-1} are characteristic Raman scattering peaks for quartz.

DISCUSSION

The petrified tree fern examined in this study displayed golden yellow to brown colors, with color variations attributed to the presence of iron oxides,

Figure 16. The Raman spectrum of petrified tree fern sample S2 shows dominantly quartz (Q) peaks with a moganite (M) peak at 503 cm^{-1}. Tiger's-eye shows the same quartz peaks but lacks the moganite peak. Spectra are offset vertically for clarity.

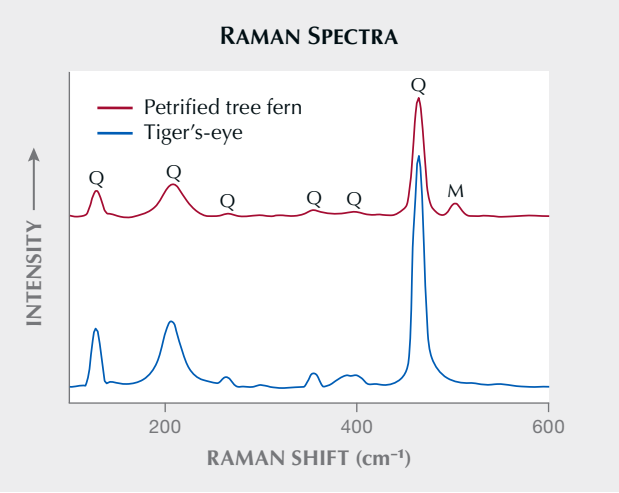

particularly hematite. Most samples were translucent to opaque, with deeper tones. Figure 12 shows the color-banded specimens resulting from the absorption of iron-bearing solutions along the wood grain. This observation suggests that the wood retains a degree of permeability (Mustoe and Acosta, 2016). Furthermore, the red and yellow exterior zones in the samples and the element mapping of iron oxide impurity minerals provide evidence that ferric oxide infiltrated the wood during the later stages of diagenesis (Saminpanya, 2016). Weathering during this process caused decomposition and subsequent recrystallization of cryptocrystalline quartz along the wood grain, reducing transparency and making the woody structure more visible (Stein, 1982; Li, 2016).

The unique characteristics of the six samples analyzed in this study, including the three-layered cortex, distinctive pith composition, the single fusiform vascular bundle, and the presence of stems embedded within an adventitious root matrix, indicated a connection to the Cretaceous tree fern *Tempskya* sp. (Clifford and Dettmann, 2005). Tree ferns are large, woody ferns that resemble trees and have trunk-like structures with fronds. The starting material of a tree fern, rather than a true tree, represents a notable variation within ordinary petrified wood.

Petrified tree fern and tiger's-eye, both being forms of quartz, bear notable similarities in appearance and physical properties. Standard gemological properties are insufficient to distinguish between them, which has led to some confusion within the jewelry market. When examined in cross section, the adventitious roots of petrified tree fern exhibited a distinct oval pattern (figure 17A), while tiger's-eye displayed a mosaic of fibrous bundles on end (figure 17B). These two patterns are very similar when viewed with the unaided eye.

In tiger's-eye, crocidolite and columnar quartz grow simultaneously from opposing crack walls toward the center of the vein during a crack-seal process. The metasomatism only occurs when oxidizing fluids break down the crocidolite to hematite and goethite (Heaney and Fisher, 2003). Fibers of crocidolite are encased within columnar quartz and when grown parallel to each other (figure 17D) (Hu and Heaney, 2010). The formation of petrified wood, on the other hand, occurs under highly specific conditions (Pakhomova et al., 2020). Early research suggested that the petrification process is often associated with volcanic activity (Murata, 1940). Fallen or still upright trees become buried by volcaniclastics due to intense geological activity (Flörke et al., 1982). Ballhaus et al. (2012) observed that trees

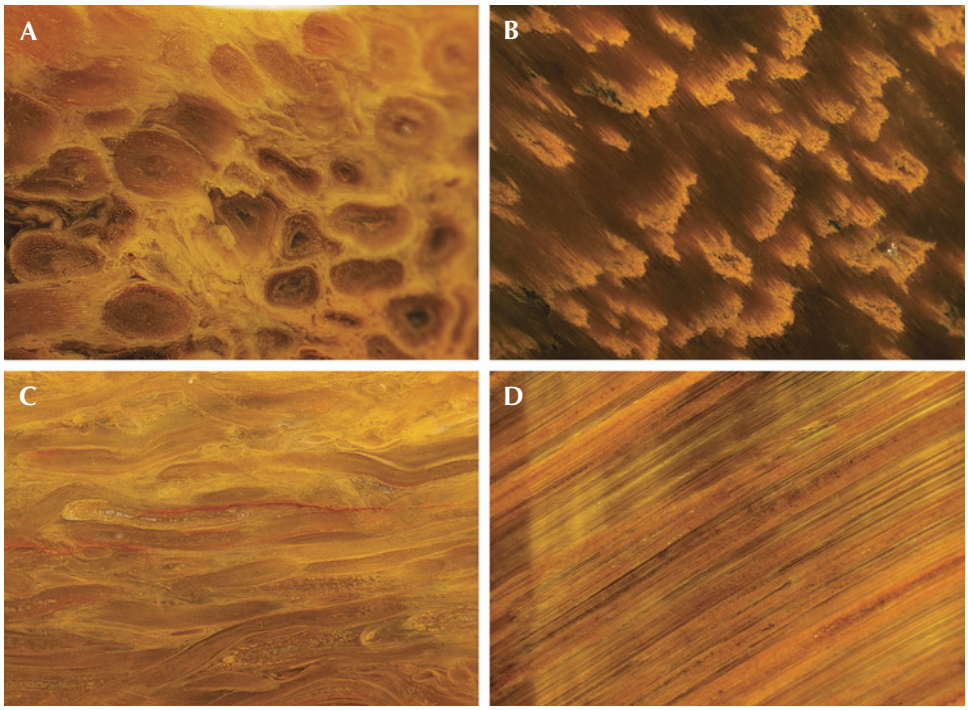

Figure 17. Comparison of surface pattern similarities between petrified tree fern and tiger's-eye. A: Adventitious roots were confined to a shallow surface layer in the cross section of sample S1. B: Under reflected light, a cross section of tiger's-eye shows tufted ends of crocidolite bundles encased within quartz. C: Adventitious roots show a relatively well-preserved circular texture in a longitudinal section. D: Tiger's-eye is characterized by a parallel fiber structure in a longitudinal section, and a silky luster is seen in polished sections. Photomicrographs by Ying Yan; fields of view 0.5 mm (A), 0.7 mm (B), 1.0 mm (C), and 1.2 mm (D).

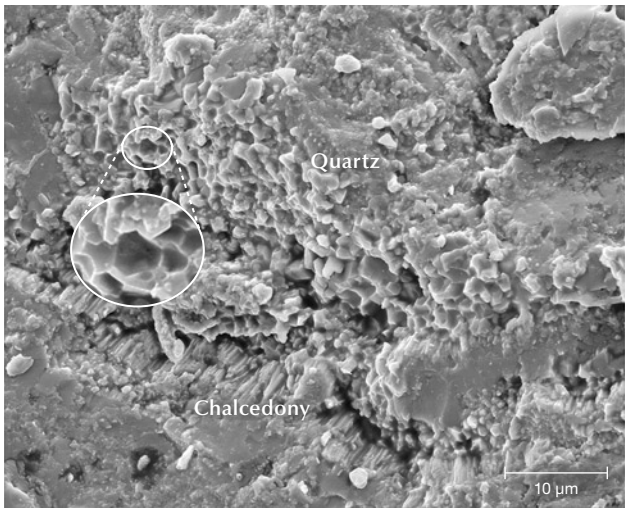

Figure 18. An SEM image of sample S3 reveals well-formed quartz particles approximately 5 µm in diameter, with a hexagonal cross section left by a fracture. Fibrous chalcedony is observed at the border transition.

exhibit a clear propensity to absorb silica from hydrothermal fluids. Over time, the minerals crystallize, preserving the original structure and morphology of the organism in a fossilized form. The primary source of silica in this process is derived from ash silts (Saminpanya, 2015). Silica is considered the most active material for petrifying wood (Scurfield and Segnit, 1984). Through this process, petrified tree fern can preserve intricate patterns of fern fronds and the overall structure of the tree fern with remarkable detail (figure 17C). Therefore, the distinct silicification processes of petrified tree fern and tiger's-eye result in unique structures and surface patterns, enabling their differentiation through careful macroscopic observation.

Buurman (1972) categorized the mineralization of wood into four processes: silicification, carbonation, phosphate accumulation, and sulfide accumulation. Among these, silicification involving quartz minerals is the most prevalent. Petrified tree fern has a chemical composition of SiO_2, and there was no significant difference in chemical composition observed among the six different samples from this study, indicating that the specimens were thoroughly silicified. Quartz plays a crucial role in preserving the cell walls, resulting in the predominantly microcrystalline quartz composition of the preserved plant structures (Dietrich et al., 2013). Cell lumina, on the other hand, are filled with cryptocrystalline silica, specifically fibrous chalcedony, occupying the areas where plant structures have disappeared. Previous studies have confirmed that the fibrous character of chalcedony may arise from various forms of silica, including moganite as a metastable phase often found in fibrous chalcedony (Hassan, 2017; Mustoe, 2023). Raman spectroscopy was used to provide further evidence of constituent phases, enabling clearer identification of moganite in petrified tree fern (Heaney and Post, 1992; Götze et al., 1998). Furthermore, the Raman spectrum of tiger's-eye lacks the signal of moganite, which might be a way to distinguish petrified tree fern from tiger's-eye.

Additionally, highly crystalline quartz exhibits a hexagonal columnar growth (figure 18). An essential preservation characteristic is the presence of open vessels that provide space for the formation of well-developed quartz after the surrounding tissue has been silicified. The quartz filling this open space results from a separate mineralization event that occurred after dissolved silica levels dropped (Mustoe, 2023). However, the large particle size and rough edges of crystalline quartz in petrified wood cause light to be reflected and refracted internally, resulting in limited transparency (Lei, 2010). Conversely, fibrous chalcedony, the primary mineral commonly found in petrified tree fern, contributes to a delicate structure and enhances transparency (Miladinović et al., 2016; Lei, 2022). Therefore, the plant pattern filled with crystalline quartz can be more clearly distinguished from the surrounding chalcedony portions. In China, chalcedony petrified tree fern is highly valued as a lapidary material and ornamental stone, with high-quality specimens sought for the creation of carvings (figure 19).

CONCLUSIONS

Petrified tree fern from northeast China exhibited colors ranging from golden yellow to brown, with additional variations attributed to the presence of iron oxides. These specimens possessed distinct plant structures such as stems, adventitious roots, and leaf traces, resulting in a unique appearance. Although standard gemological testing proved insufficient in distinguishing petrified tree fern from tiger's-eye, differences could be observed in their surface patterns, chatoyancy, and Raman spectra.

SEM-EDS and EPMA analyses confirmed the thorough silicification of the petrified tree fern samples, revealing a predominant SiO_2 composition

Figure 19. Pixiu dragon carvings are sought after in China and elsewhere; this piece carved in petrified tree fern measures approximately 35 × 20 mm. Photo by Hai-Long Wang.

across various plant structures. Additionally, SEM and Raman spectroscopy identified chalcedony as the primary mineral component in petrified tree fern. The fibrous texture of chalcedony is induced by the presence of metastable moganite, contributing to the delicate structure observed. This material is remarkable for its beautiful pattern, representing an intriguing fusion of botany and gemology.

ABOUT THE AUTHORS

Ying Yan (2009210031@email.cugb.edu.cn) is a PhD candidate, and Dr. Xiao-Yan Yu (yuxy@cugb.edu.cn, corresponding author) is a professor of gemology and mineralogy, at the School of Gemmology, China University of Geosciences in Beijing. Han-Yue Xu and Zhi-Rong Xie are postgraduate students at the School of Gemmology, China University of Geosciences in Beijing.

ACKNOWLEDGMENTS

The authors gratefully acknowledge support from China Geological Survey grant DD20190379-88 and would like to thank Dr. Ye-Ming Cheng for the meaningful discussion on botany. The authors are grateful for the insightful peer reviews of Dr. George Mustoe and Dr. Peter Heaney.

REFERENCES

Ballhaus C., Gee C.T., Bockrath C., Greef K., Mansfeldt T., Rhede D. (2012) The silicification of trees in volcanic ash - An experimental study. *Geochimica et Cosmochimica Acta*, Vol. 84, No. 1, pp. 62–74, http://dx.doi.org/10.1016/j.gca.2012.01.018

Buurman P. (1972) *Mineralization of Fossil Wood*. Rijksmuseum van Geologie en Mineralogie, Leiden.

Cheng Y.M., Liu F.X. (2017) The first discovery of Cretaceous cyatheaceae stem fossils in China. *Acta Geoscientica Sinica*, Vol. 38, No. 2, pp. 135–143.
Clifford H.T., Dettmann M.E. (2005) First record from Australia of the Cretaceous fern genus *Tempskya* and the description of a new species, *T. judithae*. *Review of Palaeobotany and Palynology*, Vol. 134, No. 1-2, pp. 71–84, http://dx.doi.org/10.1016/j.revpalbo.2004.12.001
Dietrich D., Lampke T., Rößler R. (2013) A microstructure study on silicified wood from the Permian Petrified Forest of Chemnitz. *Paläontologische Zeitschrift*, Vol. 87, No. 3, pp. 397–407, http://dx.doi.org/10.1007/s12542-012-0162-0
Flörke O.W., Köhler H.B., Langer K., Tönges I. (1982) Water in microcrystalline quartz of volcanic origin: Agates. *Contributions to Mineralogy and Petrology*, Vol. 80, No. 4, pp. 324–333.
Gao R.Q., Song Z.C. (1994) Study on Early Cretaceous palynological assemblage in deep Songliao Basin. *Acta Palaeontologica Sinica*, Vol. 33, No. 6, pp. 659–675 [in Chinese].
Götze J., Nasdala L., Kleeberg R., Wenzel M. (1998) Occurrence and distribution of "moganite" in agate/chalcedony: A combined micro-Raman, Rietveld, and cathodoluminescence study. *Contributions to Mineralogy and Petrology*, Vol. 133, No. 1, pp. 96–105, http://dx.doi.org/10.1007/s004100050440
Hardgrove C., Rogers A.D. (2013) Thermal infrared and Raman microspectroscopy of moganite-bearing rocks. *American Mineralogist*, Vol. 98, No. 1, pp. 78–84, http://dx.doi.org/10.2138/am.2013.4152
Hassan K.M. (2017) Mineralogical and geochemical signatures of silicified wood from the petrified forest, New Cairo, Egypt. *Canadian Mineralogist*, Vol. 55, No. 2, pp. 317–332, http://dx.doi.org/10.3749/canmin.1600089
Heaney P.J., Fisher D.M. (2003) New interpretation of the origin of tiger's-eye. *Geology*, Vol. 31, No. 4. pp. 323, http://dx.doi.org/10.1130/0091-7613(2003)031%3C0323:NIOTOO%3E2.0.CO;2
Heaney P.J., Post J.E. (1992) The widespread distribution of a novel silica polymorph in microcrystalline quartz varieties. *Science*, Vol. 255, No. 5043, pp. 441–443, http://dx.doi.org/10.1126/science.255.5043.441
Holden C. (2003) Tiger's eye: Looks are deceiving. *Science*, Vol. 300, No. 5617, p. 245.
Hu K.F., Heaney P.J. (2010) A microstructural study of pietersite from Namibia and China. *G&G*, Vol. 46, No. 4, pp. 280–286, http://dx.doi.org/10.5741/GEMS.46.4.280
Kim K.W., Yoon C.J., Kim P.G., Lee M.B., Lim J.H. (2010) Fine structure and X-ray microanalysis of silicified woods from a Tertiary basin Pohang, Korea by scanning electron microscopy. *Micron*, Vol. 40, pp. 519–525, http://dx.doi.org/10.1016/j.micron.2009.04.006
Kingma K.J., Hemley R.J. (1994) Raman spectroscopic study of microcrystalline silica. *American Mineralogist*, Vol. 79, pp. 269–273.
Kong H., Chen C.R., Dang Y.M., Yang J.G., Huang Q.H., Zhao C.B. (2006) Review of three Cretaceous biota in Songliao Basin. *Acta Palaeontologica Sinica*, No. 3, pp. 416–424.
Large M.F., Braggins J.E. (2004) *Tree Ferns*. Timber Press, Portland, Oregon.
Lei F.F. (2010) Mineral characteristics and gemological economic evaluation of petrified wood from Burma. Master's thesis, Guilin University of Technology [in Chinese].
——— (2022) Analysis of the influence of mineralogical characteristics of silicified wood on transparency. *Journal of Suihua University*, Vol. 42, No. 5, pp. 156–160 [in Chinese].
Li Y.T. (2016) Study on microstructure and mineralogy characteristics of petrified wood from Qitai, Xinjiang and Pagan, Myanmar. Master's thesis, China University of Geosciences, Beijing [in Chinese].
Martínez L.C.A., Olivo M.S. (2015) *Tempskya* in the Valanginian of South America (Mulichinco Formation, Neuquén Basin, Argentina)—Systematics, palaeoclimatology and palaeoecology. *Review of Palaeobotany and Palynology*. Vol. 219, pp. 116–131, http://dx.doi.org/10.1016/j.revpalbo.2015.04.002
Miladinović Z., Simić V., Jelenković R., Ilić M. (2016) Gemstone deposits of Serbia. *Geologica Carpathica*, Vol. 67, No. 3, pp. 211–222, http://dx.doi.org/10.1515/geoca-2016-0014
Murata K.J. (1940) Volcanic ash as a source of silica for the silicification of wood. *American Journal of Science*, Vol. 238, No. 8, pp. 586–596.
Mustoe G.E. (2008) Mineralogy and geochemistry of late Eocene silicified wood from Florissant Fossil Beds National Monument, Colorado. In H.W. Meyer and D.M. Smith, Eds., *Special Papers of the Geological Society of America*, Vol. 435, pp. 127–140, http://dx.doi.org/10.1130/2008.2435(09)
——— (2023) Silicification of wood: An overview. *Minerals*, Vol. 13, No. 2, article no. 206, http://dx.doi.org/10.3390/min13020206
Mustoe G.E., Acosta M. (2016) Origin of petrified wood color. *Geoscience*, Vol. 6, No. 2, article no. 25, http://dx.doi.org/10.3390/geosciences6020025
Nowak J., Florek M., Kwiatek W., Lekki J., Chevallier P., Zieba E., Mestres N., Dutkiewicz E.M., Kuczumow A. (2005) Composite structure of wood cells in petrified wood. *Materials Science and Engineering*, Vol. 25, pp. 119–130, http://dx.doi.org/10.1016/j.msec.2005.01.018
Pakhomova V., Solyanik V., Fedoseev D., Kultenko S.Y., Tishkina V.B., Gusarova V.S. (2020) Gem News International: Occurrence of petrified woods in the Russian Far East: Gemology and origin. *G&G*, Vol. 56, No. 2, pp. 306–308.
Rößler R. (2000) The late Paleozoic tree fern Parsonius- an ecosystem unto itself. *Review of Palaeobotany and Palynology*. Vol. 119, No. 1-2, pp. 143–159.
Saminpanya S. (2015) Gem News International: Thai-Myanmar petrified woods. *G&G*, Vol. 51, No. 3, pp. 337–339.
——— (2016) Trace elements and mineral chemistry of silicified wood from Thailand: Colours and elemental distribution. *Australian Journal of Earth Sciences*, Vol. 63, No. 7, pp. 873–884, http://dx.doi.org/10.1080/08120099.2016.1251492
Scurfield G., Segnit E.R. (1984) Petrifaction of wood by silica minerals. *Sedimentary Geology*, Vol. 39, pp. 149–167, http://dx.doi.org/10.1016/0037-0738(84)90048-4
Stein C.L. (1982) Silica recrystallization in petrified wood. *Journal of Sedimentary Research*, Vol. 52, No. 4, pp. 1277–1282, http://dx.doi.org/10.1306/212F8116-2B24-11D7-8648000102C1865D
Tidwell W.D., Ash S.R., Britt B.B. (2010) Oldest known dicotyledonous lianas from the early late Cretaceous of Utah and New Mexico, USA. In C.T. Gee, Ed., *Plants in Mesozoic Time: Morphological Innovations, Phylogeny, Ecosystems*. Indiana University Press, Bloomington, Indiana, pp. 271–291.
Witke L., Götze J., Rößler R., Dietrich D., Marx G. (2004) Raman and cathodoluminescence spectroscopic investigations on Permian fossil wood from Chemnitz – A contribution to the study of the permineralisation process. *Spectrochimica Acta Part A: Molecular and Biomolecular Spectroscopy*, Vol. 60, No. 12, pp. 2903–2912, http://dx.doi.org/10.1016/j.saa.2003.12.045
Xu H.Y. (2021) Mineralogy and structure characteristics of silicified tree fern from Heilongjiang. Master's thesis, China University of Geosciences, Beijing [in Chinese].
Yang X.N., Liu F.X., Cheng Y.M. (2018) A new tree fern stem, *Tempskya zhangii* sp. nov. (Tempskyaceae) from the Cretaceous of northeast China. *Cretaceous Research*, Vol. 84, No. 1, pp. 188–199, http://dx.doi.org/10.1016/j.cretres.2017.11.016
Yoon C.J., Kim K.W. (2008) Anatomical descriptions of silicified woods from Madagascar and Indonesia by scanning electron microscopy. *Micron*, Vol. 39, No. 7, pp. 825–831, http://dx.doi.org/10.1016/j.micron.2007.12.011
Yu X.Y. (2016) *Colored Gemology*, 2nd ed. Geological Publishing House, Beijing [in Chinese].